Mars Structure Service: Single-station and single-event marsquake inversion for structure using synthetic Martian waveforms. A. Khan[1], M. Drilleau[2], E. Beucler[3], M. Panning[4], P. Lognonné,[2], C. Beghein[5], H. Xu[5], S. Menina[2], S. Barkaoui[2], V.Lekic[6], S. Stähler[1], M. van Driel[1], B. Kenda[2], N. Murdoch[7], J. Clinton[1], D. Giardini[1], S. Smrekar[4], E. Stutzmann[2], M. Schimmel[8]. [1]Institute for Geophysics, ETH Zürich (Zürich, Switzerland), [2] Institut de Physique du Globe de Paris (Sorbonne Paris Cité, Université Paris Diderot, CNRS F-75005 Paris, France), [3]Université de Nantes, Laboratoire de Planétologie et de Géodynamique (UMR-CNRS 6112, Nantes, France), [4]Jet Propulsion Laboratory, California Institute of Technology (Pasadena, CA 91109, USA) [5]Department of Earth, Planetary, and Space Sciences, University of California Los Angeles (Los Angeles, CA 90095, USA), [6]Department of Geology, University of Maryland (College Park, MD 20742, USA), [7]ISAE-SUPAERO (Toulouse University, 10 Ave E. Belin, 31400 Toulouse, France), [8]ICTJA-CSIC (Barcelona, Spain).

Introduction: The InSight lander successfully delivered a geophysical instrument package on the Martian surface on November 26th, 2018, including a broadband and a short-period seismometer (Seismic Experiment for Interior Structure, SEIS). The seismic instrument package is specifically designed to record marsquakes and meteoritic impacts in Martian conditions **[1]**. Routine operations are split into two services: the Mars Structure Service (MSS) and the Marsquake Service (MQS that are responsible for defining structure models and seismicity catalogs, respectively **[2, 3]**.

The first "deliverable" of the MSS will be a model based on the events detected during the first 3 months of seismic monitoring of the mission, for which only a few quakes might be expected based on current estimates of Mars seismic activity. To test our approach of determining the interior model of Mars and to prepare the InSight science team for data return, we made use of a "blind test" time series for which the Marsquake parameters (location, depth, origin time, and moment tensor) and interior model were unknown to the group at large.

Blind test data: In preparation for the mission, the goal was to develop mature algorithms to handle the data as efficiently as possible. Synthetic seismic waveforms were computed in a 1D mantle model with a 3D crust on top using AxiSEM **[4]** and Salvus **[5]**. Time series were created by adding seismic noise based on pre-landing estimates of the instrument at the landing site. It includes noise generated by the sensors and electronic system, environment, and nearby lander **[6, 7, 8]**.

To characterize what we could learn about Mars interior structure with a single station and a single (first) seismic event, we performed inversions of synthetic data following a "blind test" process, where the interior model was unknown to all involved team members.

Inversion methods: We detail and compare the results of this "blind test" using 4 different methods that we shall abbreviate MD, EB, CH, and AK, respectively. The inversions rely mostly on Bayesian techniques to obtain robust estimates of interior structure parameters. The methods include inversion of surface wave dispersion data (EB), body waves and surface waves arrival times (MD and AK), and waveforms (CH).

Effects of fixing marsquake location and origin time are investigated, as is the effect of using a fixed vs. flexible Vs parameterizations. To allow for tighter constraints, we also test the use of thermodynamically-constrained priors (AK) **[9]**.

Results: Vs profiles retrieved by each of the 4 methods are shown in figure **1**, where mean Vs profiles and associated standard deviation are shown in figure **2a**. A strong feature common to all the distributions is a mean Vs value of approximately 3.2 km/s in the first 40 to 80 km (figure **2a**).

The MD distribution (figure **1a**) is fairly spread out compared to the model solution ranges, because location and origin time of the quake is also inverted for. Between 60 and 120 km a bimodal distribution is observed which should indicate the presence of a discontinuity, but its location is not clearly constrained. The distribution of the EB and CH methods (figures **1b** and **1c**) are narrower because the location and origin time of the quake are fixed to the MQS estimate. The EB and CH methods retrieve discontinuities at 45 and 65 km, respectively, which are considered representative of the Moho discontinuity. The results of the AK method (figure **1d**) show a stronger discontinuity between 60-80 km depth and a shallower discontinuity near 10 km depth. Model variability is clearly more constrained in the case of AK and reflects the tight bounds imposed by thermodynamic constraints.

The differential arrival times between minor-arc Rayleigh wave group arrivals and the P wave arrival for the sampled models of each method are displayed in figure **2b**. The values are in good agreement between 10 and 40 s, but diverge at longer period.

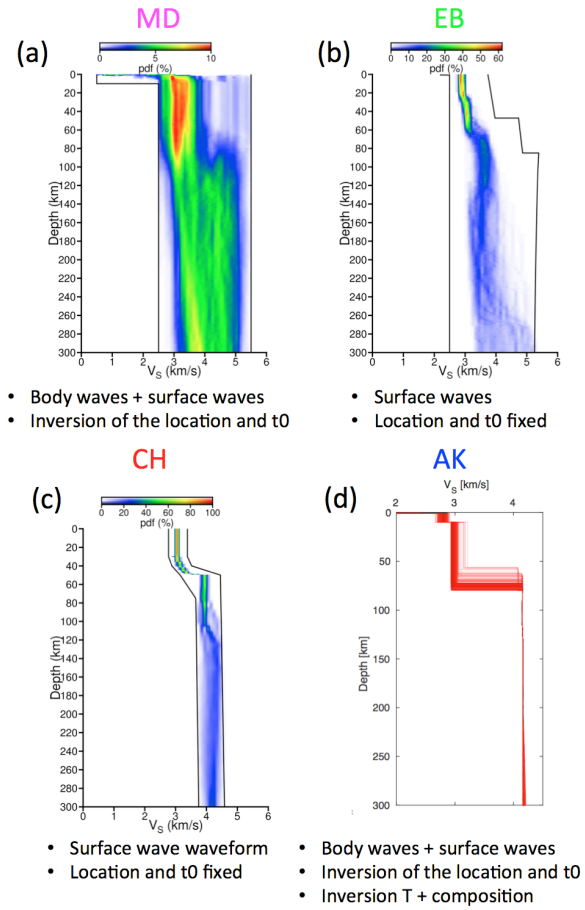

Figure 1. Probability density functions of the Vs profiles as a function of depth for 4 different methods developed by the MSS. Blue and red values in (a)-(c) show low and high probability density, respectively. Black lines correspond to the minimum and maximum allowed values. Models plotted in (d) show all accepted models.

Discussion: While there is good agreement between the mean velocity profiles across the different methods developed by the MSS, there is less agreement on depth and magnitude of a discontinuity. These differences reflect a number of issues in the inversion process: (1) variable vs. fixed source parameters; (2) type of seismic data used; (3) choice of parameterization and prior information; and finally (4) definition of misfit function.

The techniques considered here form the core part of the planned modeling of the MSS that will be ultimately employed with the first recording of a seismic event by InSight. The true model used to build the "blind test" data will be available soon to finalize our comparison review.

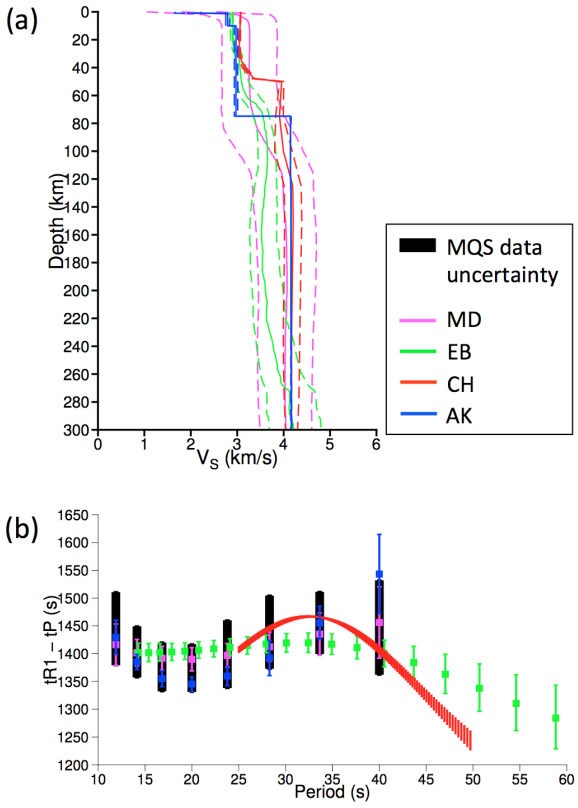

Figure 2. (a) Mean Vs profiles (solid lines) and standard deviation (dashed lines) for each of the distributions shown in Figure 1. (b) Mean and standard deviation of the differential travel time between minor-arc Rayleigh wave group arrival times and P wave arrival time as a function of period for each method. Observations (based on MQS measurements) are shown in black.

References: [1] Lognonné et al. (2018) *Space Sci. Rev, 214*. [2] Panning et al. (2017) *Space Sci. Rev, 211,* 611–650. [3] Clinton et al. (2018) *Space Sci. Rev., 214,* 133. [4] Nissen Meyer et al. (2014) *Solid Earth, 5,* 425–445. [5] Afanasiev et al. (2018) *GJI, 216,* 1675–1692. [6] Murdoch et al. (2017a) *Space Sci. Rev, 211,* 457–483. [7] Murdoch et al. (2017b) *Space Sci. Rev, 211,* 429–455. [8] Kenda et al. (2017a) *Space Sci. Rev, 211,* 501–524. [9] Khan et al. (*2016) Phys Earth Planet. Int., 258*, 28-42.